A novel totivirus alters gene expression and vacuolar morphology in *Malassezia* cells and induces a TLR3-mediated inflammatory immune response

Minji Park[a], Yong-Joon Cho[b], Donggyu Kim[c], Chul-Su Yang[c,d], Shi Mun Lee[e], Thomas L. Dawson Jr.[e,f], Satoshi Nakamizo[e], Kenji Kabashima[e,g], Yang Won Lee[h,i], Won Hee Jung [a,#]

[a]Department of Systems Biotechnology, Chung-Ang University, Anseong, 17546, Korea

[b]The Research Institute of Basic Sciences, Seoul National University, Seoul, 08826, Korea

[c]Department of Molecular and Life Science, Hanyang University, Ansan 15588, Korea

[d]Department of Bionano Technology, Hanyang University, Seoul, 04673, Korea

[e]Singapore Immunology Network (SIgN) and Skin Research Institute of Singapore (SRIS), Agency for Science, Technology and Research (A*STAR), 8A Biomedical Grove, IMMUNOS Building, Biopolis, 138648 Singapore

[f]Center for Cell Death, Injury & Regeneration, Departments of Drug Discovery & Biomedical Sciences and Biochemistry & Molecular Biology, Medical University of South Carolina, Charleston, SC, 29425, United States

[g]Department of Dermatology Kyoto University Graduate School of Medicine, Kyoto, 606-8507, Japan

[h]Department of Dermatology, School of Medicine, Konkuk University, Seoul, 05029, Korea

[i]Research Institute of Medicine, Konkuk University, Seoul, 05029, Korea

Running Head: A novel totivirus in *Malassezia*

#Address correspondence to Won Hee Jung, whjung@cau.ac.kr

Word counts

Abstract: 206 words; Text: 4,730 words

Abstract

Most fungal viruses have been identified in plant pathogens, whereas the presence of viral particles in human pathogenic fungi is less well studied. In the present study, we observed extrachromosomal double-stranded RNA (dsRNA) segments in various clinical isolates of *Malassezia* species. *Malassezia* is the most dominant fungal genus on the human skin surface, and species in this group are considered to be etiological factors in various skin diseases including dandruff, seborrheic dermatitis, and atopic dermatitis. We identified novel dsRNA segments and our sequencing results revealed that the virus, named MrV40, belongs to the *Totiviridae* family and contains an additional satellite dsRNA segment encoding a novel protein. The transcriptome of virus-infected *M. restricta* cells was compared to that of virus-free cells, and the results showed that transcripts involved in ribosomal biosynthesis were down regulated and those involved in energy production and programmed cell death were increased in abundance. Moreover, transmission electron microscopy revealed significantly larger vacuoles for virus-infected *M. restricta* cells, indicating that MrV40 infection dramatically altered *M. restricta* physiology. Our analysis also revealed that a viral nucleic acid from MrV40 induces a TLR3-mediated inflammatory immune response in bone marrow-derived dendritic cells (BMDCs) and this result suggests that a viral element contributes to the pathogenesis of *Malassezia*.

Importance

Malassezia is the most dominant fungal genus on the human skin surface and is associated with various skin diseases including dandruff and seborrheic dermatitis. Among *Malassezia* species, *M. restricta* is the most widely observed species on the human skin. In the current study, we identified a novel dsRNA virus, named MrV40, in *M. restricta* and characterized the sequences and structure of the viral genome along with an independent satellite dsRNA viral segment. Moreover, we found altered expression of genes involved in ribosomal synthesis and programmed cell death, indicating that virus infection altered the physiology of the fungal host cells. Our data also showed that the viral nucleic acid from MrV40 induces a TLR3-mediated inflammatory immune response in bone marrow-derived dendritic cells (BMDCs), indicating that a viral element likely contributes to the pathogenesis of *Malassezia*. This is the first study to identify and characterize a novel mycovirus in *Malassezia*.

Introduction

Viruses have been observed in many fungal species since their first identification in mushrooms (1). Fungal viruses, also known as mycoviruses, possess different forms of viral genomes including double-stranded RNA (dsRNA), single-stranded RNA (ssRNA), and single-stranded DNA (ssDNA). It is estimated that 30–80% of all fungal species, mainly endophytic fungi, are infected with viruses. Unlike viruses that infect other organisms, the transmission of fungal virus occurs vertically by cell division or horizontally via mating or hyphal anastomosis, with no extracellular phase of the virus life cycle. dsRNA segments have predominantly been found for fungal viruses and, taxonomically, the fungal dsRNA viruses are classified into seven families: *Chrysoviridae*, *Endornaviridae*, *Megabirnaviridae*, *Quadriviridae*, *Partitiviridae*, *Reoviridae*, and *Totiviridae* (2).

The model fungus *Saccharomyces cerevisiae* also carries a dsRNA virus that belongs to the *Totiviridae* family and is known as the L-A virus. A unique feature of fungal viruses of the *Totiviridae* family is their capability to produce the killer toxin that lyses susceptible neighbor strains, whereas the virus-containing strain (also known as a killer strain) is immune to the toxin. Studies of how the virus produces killer toxins in *S. cerevisiae* showed that killer toxins are encoded by a satellite dsRNA segment, known as the M satellite, within the L-A virus. To date, four different killer toxins, K1, K2, K28, and Klus have been described (3-6). The *S. cerevisiae* L-A virus forms icosahedral particles with a diameter of approximately 39 nm (7). The virus possesses a non-segmented 4.6-kb dsRNA genome consisting of two open reading frames (ORFs), *gag* and *pol*, which overlap by 130 base pairs (bp) (8). *gag* encodes a major 76-kDa capsid protein (CP), and a 180-kDa minor protein species is encoded as a Gag-Pol fusion protein by a −1 ribosomal frame-shift event (9, 10). The C-terminus of the Gag-Pol

fusion protein possesses viral RNA-dependent RNA polymerase (RDRP) activity (8). The ribosomal frameshift is an interesting feature in a compact viral genome and has been commonly found in various viral genomes as a mechanism to allow viruses to express overlapping ORFs. Studies of *S. cerevisiae* L-A virus revealed that the mechanism of frameshifting is based on the sequence structures including a canonical slippery heptamer, 5′-X XXY YYZ-3′ (X= A, U or G; Y=A or U; Z=A, U, or C) and RNA pseudoknot (11).

Fungal viruses have also been considered as biocontrol agents in the field of agriculture. For example, a virus causes hypovirulence in the chestnut blight fungus *Cryphonectria parasitica* (12, 13), and a virus mediates the biocontrol of other phytopathogenic fungi such as *Helminthosporium victoriae*, *Sclerotinia sclerotiorum*, and *Botrytis cinerea* (14).

Although viral infections in fungal cells are widespread, the interactions between the fungal virus and its host are not well understood. One of the most studied host defense mechanisms is RNA silencing. Several studies have shown that RNA silencing functions as an antiviral defense mechanism against *C. parasitica* in fungi. Disruption of the dicer pathway in *C. parasitica* increases the susceptibility to virus infections (15), and p29 was identified as a suppressor that inhibits expression of the genes required for RNA silencing-mediated viral defense in the fungus (16). Similarly, conserved RNA silencing-mediated antiviral defense systems have been identified in *Aspergillus nidulans*, *Rosellinia necatrix*, and *Fusarium graminearum* (17-19).

Malassezia is the most dominant fungal genus on the human skin surface and is considered as an etiological factor in various skin diseases including dandruff, seborrheic dermatitis, and atopic dermatitis (20-23). Eighteen *Malassezia* species have been identified; among them, *M. restricta* is the most abundant on the human skin (20). Recent studies showed an increased

burden of *M. restricta* on the scalp of patients with dandruff, indicating an association between dandruff and the fungus although its role as a pathogenic organism is still unclear, and the host susceptibility should be taken into consideration (21, 24-27). Most fungal viruses are found in plant pathogenic fungi, whereas few examples of viral particles have been identified in human pathogenic fungi such as *Candida albicans* (28). In the present study, we observed extrachromosomal dsRNA segments in various *M. restricta* clinical isolates which represented a novel viral genome and its satellite. Sequence analysis revealed that the virus belongs to the *Totiviridae* family and that the additional satellite dsRNA segment encodes a novel protein. The interactions between the viral elements and the fungal host, and the impact of the virus on fungal interactions with immune cells were evaluated.

Results

Identification of extrachromosomal dsRNA segments in *Malassezia*

Extrachromosomal nucleic acid bands were observed in total nucleic acid extracts of the *M. restricta* strains isolated in our recent study (29). Among the strains, *M. restricta* KCTC 27540 was used to identify extrachromosomal segments. Total nucleic acids were extracted from the strain and digested with DNase I, RNase A, and RNase T1. The extrachromosomal segments and ribosomal RNA were resistant to DNase I, indicating that they were neither ssDNA nor dsDNA. RNase A degraded all nucleic acids except for genomic DNA, whereas RNase T1, which catalyzes the degradation of ssRNA, removed ribosomal RNA only (30). These results suggested that the extrachromosomal segments correspond to dsRNA, and that *M. restricta* KCTC 27540 possesses two separate extrachromosomal segments estimated by agarose gel electrophoresis to be approximately 4.5 and 1.5 kb (Fig. 1A).

To confirm whether the extrachromosomal segments observed in other *M. restricta* clinical isolates were also dsRNA, total nucleic acid extracts from the strains other than *M. restricta* KCTC 27540 were treated with DNAse I and RNase T1. The extrachromosomal segments remained unaffected after enzyme treatment, indicating that they are also dsRNA, as in *M. restricta* KCTC 27540 (Fig. 1B). Moreover, other *Malassezia* species including *M. globosa*, *M. pachydermatis*, and *M sympodialis* showed similar extrachromosomal dsRNA segments suggesting that these segments are common characteristics of *Malassezia* species (Fig. 1C). Agarose gel electrophoresis revealed extrachromosomal segments composed of at least two separate dsRNA fragments except for *M. restricta* KCTC 27543, which showed a single dsRNA fragment. Additionally, the large fragments of dsRNA showed similar sizes (~5.0 kb), whereas the small dsRNA segments varied in size in different strains (Fig. 1B and 1C). We hypothesized that the dsRNA segments from *Malassezia* strains represent the dsRNA elements of mycoviruses, which are prevalent in all major fungal taxa (2).

Sucrose gradient ultracentrifugation was conducted to purify virus particles to confirm that the dsRNA segments in the *Malassezia* strains were indeed viral elements. The separated nucleic acids and proteins in each fraction were analyzed. Two dsRNA fragments (~5.0 and ~1.7 kb) were clearly visible in fractions 1–6 following agarose gel electrophoresis (Fig. 2A). Moreover, the results of sodium dodecyl sulfate-poly acrylamide gel electrophoresis (SDS-PAGE) showed that fractions 3–6 contained protein bands with an estimated molecular weight of ~77 kDa (Fig. 2B). This molecular weight is similar to that of the known capsid protein of the *S. cerevisiae* mycovirus (9, 31, 32). Fractions 3–6 were subsequently evaluated by microscopy to visualize mycovirus particles in *M. restricta*. Transmission electron microscopy (TEM) images showed virus-like particles with an isometric shape and a

diameter of 43 nm (Fig. 2C). These results support the hypothesis that the extrachromosomal dsRNA segments formed the genome of mycovirus in *M. restricta* KCTC27540. We named the viral particle as MrV40 (*M. restricta* KCTC 27540 Mycovirus). The large and small dsRNA viral fragments were named as MrV40L and MrV40S, respectively. In addition to evaluating images of the purified virus particle, we examined the morphology of *M. restricta* KCTC27540 cells containing the mycovirus for comparison with virus-free cells of *M. restricta* KCTC 27527 by TEM. The results showed that, in general, the size of vacuoles in the virus-containing strain was significantly larger than those in the virus-free strain, suggesting that the virus influences vacuole size in *M. restricta* (Fig. 3).

Determination of dsRNA sequence of MrV40L

The complete sequence of MrV40L was determined by a combination of the Illumina MiSeq technique and the Sanger sequencing method using purified viral dsRNA. The length of the complete assembled sequence of MrV40L was 4,606 bp, and two overlapping open reading frames (ORFs), designated as ORF1 and ORF2, were identified (Fig. 4A). ORF1 corresponds to the region from nucleotides (nt) 28 to 2,097 and encodes a polypeptide of 689 amino acids with a molecular weight of 77 kDa. ORF2 corresponds to the region from nt 1,949 to 4,538 and encodes a polypeptide of 862 amino acids with a molecular weight of 98 kDa. The results of BLAST analysis showed that the protein sequences of ORF1 and ORF2 were highly similar to the capsid protein (CP; the Pfam families of LA-virus_coat, PF09220) and viral RNA-directed RNA polymerase (RDRP; the Pfam family of RDRP_4, PF02123) of *S. segobiensis* virus L belonging to the genus *Totivirus* (Totiviridae family) with 53% (YP_009507830.1) and 52% (YP_009507831.1) identities, respectively (33). Eight conserved

179 motifs, which are commonly found in totiviruses, were found within ORF2, supporting the
180 classification of MrV40 as a totivirus (Fig. 4B) (34). Moreover, phylogenetic analysis with
181 known amino acid sequences of RDRP of dsRNA mycoviruses demonstrated that the RDRP
182 encoded by the MrV40L genome was clustered with totiviruses (Fig. 4C). Thus, MrV40L is a
183 dsRNA viral genome encoding CP and RDRP, and we propose that MrV40 belongs to the
184 *Totivirus* genus.

185 Next, we analyzed the genomic sequences of dsRNA viruses in other clinical *M. restricta*
186 isolates to confirm that they were similar to those of MrV40L, and thus belong to the
187 *Totivirus* genus. RT-PCR was performed using four primer sets corresponding to the sequence
188 of the conserved regions of CP and RDRP in the MrV40L genome (Fig. 5A). The results
189 showed that six of 11 viruses generated RT-PCR products, suggesting the presence of viral
190 genomes similar to MrV40Ls, while the remaining samples had dissimilar viral genomes (Fig.
191 5B).

192 Furthermore, we performed phylogenetic classification of the same viruses found in other
193 clinical *M. restricta* isolates by multilocus sequence typing of the 1,075-bp region, 638 bp of
194 ORF1, and 437 bp of ORF2, corresponding to *gag* and *pol*, respectively, within the viral
195 genomes. The results revealed that the viruses were classified into three clades: clade I
196 (MrV12L, MrV16L, MrV40L, MrV79L, MrV80L, and MrV82L), clade II (MrV18L,
197 MrV43L, MrV83L, and MrV50L), and clade III (MrV24L) (Fig. 5C). Additionally, the
198 sequences of the 1,075-bp region of MrV40L, MrV79L, and MrV82L in the clade I were 100%
199 identical, suggesting that they originated from the same lineage.

200

201 **Determination of dsRNA sequence of MrV40S**

To determine the sequence of MrV40S, the dsRNA segments of MrV40S were extracted from agarose gels and then subjected to cDNA cloning and sequencing (See Materials and Methods). Using the partial sequences obtained from cDNA clones and the sequences obtained from repeated 5′ rapid amplification of cDNA ends (RACE), we successfully determined the complete sequence of MrV40S. The sequence of MrV40S was 1,355 bp, and a single ORF was identified in the 3′ region (from nt 773 to 1,097) which encoded a polypeptide of 124 amino acids with a molecular weight of 15.6 kDa. The ORF was designated as ORF3. Although we obtained the complete sequence of MrV40S, no homologous protein sequence was identified by BLAST analysis using all currently available databases.

Mycoviruses belonging to totivirus, particularly the *S. cerevisiae* LA-virus, often possess a satellite dsRNA segment known as M dsRNA, which is responsible for producing a killer toxin that excludes neighboring yeast cells. Because MrV40L resembles M dsRNA, we predicted that MrV40S produces a protein that inhibits other *Malassezia* strains and/or other fungal and/or bacterial cells residing on the skin. To test the toxin-like activity of the protein produced from MrV40S, ORF3 was cloned and the protein was heterologously expressed in *Escherichia coli* and purified (Fig. 6A). The activity of the purified protein was evaluated against several pathogenic fungi and bacteria including *M. restricta*, *C. albicans*, *Cryptococcus neoformans*, *E. coli*, and *Staphylococcus aureus*. Unexpectedly, the purified protein displayed no growth inhibitory effect on the microbial cells tested (data not shown). Based on these results, we concluded that the novel protein produced from ORF3 likely has no toxin-like activity against the microorganisms tested, and further functional studies are required to characterize its function.

M dsRNA in *S. cerevisiae* produce several variants of killer toxins, M1, M2, M3, and Mlus, and they showed limited homology in their protein sequences (4-6). Based on this information, we compared the sequences of satellite dsRNA genomes between MrV40S and that in other *M. restricta* strains containing the small dsRNA segments. Reverse transcription (RT)-PCR was conducted using a series of primers specific to MrV40S. The results suggested that among the nine strains tested, only the satellite dsRNA in *M. restricta* KCTC 27582 possessed a similar dsRNA segment. These data indicate that the satellite dsRNA genome sequences are highly variable (Fig. 6B).

MrV40 altered transcriptome profiles in the host *M. restricta* strain

To understand the influence of MrV40 on the host physiology, we sequenced and compared the transcriptomes of *M. restricta* KCTC27540 containing MrV40 and a strain sterilized by numerous serial passages, named as the virus-cured strain (see Materials and Methods, and Fig. S1). Transcriptome analysis showed that 258 and 809 genes were up- and down-regulated by more than 2-fold, respectively, in the virus-infected strain compared to the virus-cured strain (Table 1 and Table S1). These results indicate that the presence of the virus may impact a number of physiological processes in *M. restricta*.

In *S. cerevisiae*, numerous genes are known to be involved in maintaining its dsRNA virus (35) and are categorized into two groups: *MAK* (maintenance of killer) and *SKI* (superkiller). At least 25 *MAK* genes have been reported (36); among them, *MAK3*, *MAK10*, and *PET18* were shown to be required for the maintenance of both *S. cerevisiae* L-A virus and its M satellite, whereas all other *MAK* genes are responsible only for the M satellite (37-42). We couldn't find the homologs of *MAK10* or *PET18* in the genome of *M. restricta*, suggesting

that a different or modified virus maintenance mechanism may be present in the fungus compared to *S. cerevisiae* (Table 2). The results also showed that among the *MAK* homologs, *MAK1*, *MAK5*, *MAK11*, *MAK16*, *MAK21*, *MAK7*, and *MAK8* were downregulated by more than 2-fold. In *S. cerevisiae*, these genes, except for *MAK1*, were involved in 60S ribosomal subunit biosynthesis and M satellite maintenance. Thus, we predicted that MrV40 reduced ribosomal biogenesis within the host. Additionally, *M. restricta* contained a series of *SKI* homologs. However, no genes were differentially expressed in *M. restricta* KCTC27540 containing MrV40 compared to the virus-cured strain, indicating that the function of *SKI* genes was not critical for maintaining the virus.

In addition to the genes involved in virus maintenance, we observed upregulation of numerous genes required for the TCA cycle and the electron transport chain, including MRET_1104 (NADH dehydrogenase (ubiquinone) Fe-S protein 7), MRET_1378 (succinate dehydrogenase (ubiquinone) iron-sulfur subunit), MRET_1953 (NADH dehydrogenase (ubiquinone) Fe-S protein 1), MRET_2042 (fumarate hydratase, class II), MRET_2097 (succinate dehydrogenase (ubiquinone), MRET_2956 (2-oxoglutarate dehydrogenase E1 component), MRET_3173 (dihydrolipoamide dehydrogenase) and MRET_4117 (aconitate hydratase) (Table 3). These results suggest that virus maintenance and propagation may require higher energy production in the host cell.

The overall dysregulation of primary metabolism may disturb the normal cell physiology in the *M. restricta* strain infected with MrV40. Indeed, we observed up-regulation of genes involved in programmed cell death in the fungal host cells. For example, the expression of MRET_3200 (p38 MAP kinase), MRET_1134 (programmed cell death 6-interacting protein), and MRET_2499 (autophagy-related protein, *ATG101*), which are associated with programmed cell death, was upregulated by 4.43-, 3.14-, and 2.83-fold in the virus-infected

fungal cells, respectively. Moreover, MRET_0103 (FAS-associated factor), which is involved in Fas-induced cell death, was found to be strongly upregulated (8.80-fold) in the presence of the virus within the fungal host (43). It is well-known that programmed cell death is triggered during virus infection (44, 45), and our findings agree with this observation. Differential expression of numerous genes involved in energy metabolism and programmed cell death may have influenced the abnormally larger vacuole in the MrV40-containing strain observed by TEM (Fig. 3C).

MrV40 induced the TLR3-mediated immune system

Since it was first reported that fungal viral dsRNA induces cytokine production in rabbits (46-48), several studies have demonstrated that Toll-like receptor 3 (TLR3) plays a central role in viral dsRNA recognition and production of inflammatory cytokines in innate immune cells (49, 50). Additionally, a recent study showed that *S. cerevisiae* viral dsRNA stimulates the immune system through TLR3 in a human embryonic kidney cell line (51). We therefore investigated whether MrV40 itself or the virus-containing *Malassezia* cells alter the expression patterns of TLRs and cytokine production in mammalian cells. To this end, bone marrow-derived dendritic cells (BMDCs) obtained from C57BL/6 mice, which have been used as a model to study the interactions between fungal cells, including *Malassezia*, and the innate immune system in a mammalian host (52, 53), were used in our study.

Purified MrV40 dsRNA, capsid protein of MrV40, total cell lysates of virus-infected *M. restricta* strains (KCTC 27540 and KCTC 27550), and virus-free *M. restricta* strains (KCTC 27527 and KCTC 27539) were co-incubated with BMDCs, and the expression of TLRs and cytokines were analyzed. First, we found that TLR3 expression was significantly induced by

295 purified dsRNA, whereas the expression of other TLRs were unchanged. These results were
296 supported by observation of highly increased expression of TLR3 in the cell lysates of the
297 virus-infected *Malassezia* strains KCTC 27527 and KCTC 27539 compared to virus-free
298 strains. However, the purified capsid protein from MrV40 did not alter the expression level of
299 any TLR, indicating that dsRNA, but not the capsid protein, induced *TLR3* expression (Fig.
300 7A).

301 We also evaluated the expression of several inflammatory cytokines including tumor necrosis
302 factor (TNF)-α, interleukin (IL)-6, IL-10, interferon (IFN)-α and IFN-γ, in response to
303 MrV40 dsRNA, capsid protein, and *M. restricta* cell extracts with or without the virus.
304 Particularly, IFN-α and IFN-γ were examined because they are known to be involved in the
305 antiviral response in mammals (54). The results of the cytokine analysis indicated that
306 purified MrV40 dsRNA and the cell extracts of the *M. restricta* strains containing the virus
307 showed significantly increased production of all cytokines tested. However, a relatively small
308 increase was observed in BMDCs treated with purified capsid protein, suggesting that the
309 MrV40 capsid contributes to cytokine production, but the contribution of the protein is
310 marginal (Fig. 7B). Cytokine profiles were also measured in homozygous *TLR3* knockout
311 mice, as our observations suggested a connection between TLR3 and cytokine production
312 upon MrV40 treatment. As shown in Fig. 7B, compared to wild-type BMDCs, cytokine levels
313 in BMDCs isolated from *TLR3* knockout mice were not significantly altered. These data
314 suggest that increased production of the cytokines TNF-α, IL-6, IL-10, IFN-α, and IFN-γ in
315 response to MrV40 was TLR3-dependent in BMDCs. Our data also showed that the MrV40
316 capsid proteins caused a marginal increase in cytokine expression in both wild-type and *TLR3*
317 knockout BMDCs, indicating that the response to the viral capsid is TLR3-independent.

318 Notably, small increases in the production of TNF-α and IFN-α in *TLR3* knockout mice in
319 response to the cell extract of virus-infected *M. restricta* KCTC 27540 were ignored in our
320 results because only one sample among the two virus-infected strains displayed an increase.
321 The change in IL-10 in the same mutant BMDCs was also excluded because the differences
322 were statistically insignificant. Overall, our data suggest that dsRNA in MrV40 triggers an
323 increase in the production of cytokines involved in inflammation and that TLR3 plays a
324 central role in the host response.

325

326 **Discussion**

327 In the current study, we detected dsRNA virus in several clinical isolates of *Malassezia*
328 species. Among them, MrV40 identified in *M. restricta* KCTC 27540 was selected, and its
329 genome structure, effects on host gene expression, and influence on the mammalian immune
330 response were evaluated. Our data showed that MrV40 consists of two RNA segments, which
331 we named as MrV40L and MrV40S. The results of genome sequence analysis suggested that
332 these segments were 4,606 and 1,355 bp, respectively, and belong to the totivirus. Typically,
333 the genomes of the viruses belonging to the genus *Totivirus* consist of non-segmented dsRNA
334 with sizes between 4.6 and 7.0 kb, and contain two ORFs, *gag* and *pol*. Studies have
335 specifically examined the genome structure of *Totivirus* because of the overlapping nature of
336 the two ORFs, where a -1 frameshift occurs, resulting translation of the fusion protein (2).
337 The overlapping ORFs and frameshift were frequently observed in a compact viral genome to
338 translate proteins and were found in several dsRNA and ssRNA viruses; these ORFs allow
339 ribosomes to translate CP and RDRP continuously with a missing CP termination codon (11,
340 55, 56). It was reported that the mechanism of frameshifting in the viral genome is based on

the pseudoknot structure of the mRNA for efficient slipping via a slippery site (57). For example, in the genome of the *S. cerevisiae* L-A virus, the 5′ ORF (*gag*) encodes a 76-kDa CP and the 3′ ORF (*pol*) encodes an RDRP which is expressed as a 180-kDa CP-RDRP fusion protein generated by a -1 ribosomal frameshift (8, 11). In our study, MrV40L (the major dsRNA segment in MrV40) contained two overlapping ORFs, ORF1 and ORF2. We identified a putative slippery site heptamer, 5′-GGGTTTT-3′, at the region from nt 1, 968 to 1,974 for the -1 ribosomal frameshift, which may be associated with production of the fusion protein of 170 kDa in MrV40L. A previous study suggested that in the *S. cerevisiae* L-A virus, the rate of ribosomal frameshifs was approximately 1.8%, giving 120 CP and 2 CP-RDRP fusion protein molecules per virus particle (11). Considering the low efficiency of producing the fusion proteins by ribosomal frameshifting, we expected to observe a significantly lower translation rate of the fusion protein; indeed, the putative 170-kDa band was not detected by SDS-PAGE. In addition to MrV40L, we determined the sequence of the satellite dsRNA segment MrV40S and found that it consists of 1,355 nt containing a single ORF, ORF3, producing a novel 15.6-kDa protein. As observed for other totiviruses, the possible toxin-like activity of the protein was investigated in our study, but no growth inhibitory activity against several bacteria and fungi was observed.

It has been estimated that 30–80% of fungal species in nature are infected with viruses, and a fungal host normally shows no specific symptoms upon infection (14). However, several genes were shown to be required for maintaining and propagating viruses in the host fungal cells. In *S. cerevisiae*, numerous chromosomal genes are known to be involved in viral propagation and expression of the viral killer toxin (35). Furthermore, several genes are known to be responsible for maintaining the L-A virus and M dsRNA in *S. cerevisiae*. The *MAK* genes are required for the propagation and maintenance of the L-A virus and M dsRNA

in *S. cerevisiae* (58). Among the *MAK* genes, *MAK3*, *MAK10*, and *PET18* are required for the maintenance of both L-A virus and M dsRNA, whereas all other *MAK* genes are responsible only for M dsRNA (37-42). Particularly, *MAK3* encodes an N-acetyltransferase and is required for N-acetylation of the coat protein (37, 59). A previous study showed that the coat proteins without acetylation failed to self-assemble, resulting in the loss of all dsRNA viruses (38). *MAK10* and *PET18* (*MAK30+MAK31*) encode a non-catalytic subunit of N-terminal acetyltransferase and a protein of unknown function, respectively. Mutant strains lacking each gene contained unstable viral particles, indicating that the genes are involved in the structural stability of LA-virus and M dsRNA (39). *MAK1* (*MAK17*, *TOP1*) encodes DNA topoisomerase I, and other *MAK* genes including *MAK2*, *MAK5*, *MAK11*, *MAK16*, *MAK21*, *MAK7* (*RPL4A*), *MAK8* (*TCM1*), and *MAK18* (*RPL41B*) are related to 60S ribosomal subunit assembly (42, 60, 61). All mutant stains lacking the above genes showed decreased levels of free 60S ribosomal subunits and the inability to maintain M dsRNA, suggesting that stable propagation of the satellite dsRNA depends on 60S ribosome synthesis (41, 42). In addition to the *MAK* genes, the *SKI* gene family has been shown to be involved in the maintenance and propagation of virus in *S. cerevisiae*. *SKI1* (*XRN1*) encoding a 5′-3′ exonuclease is involved in the degradation of uncapped mRNA including viral mRNA, and *SKI2*, *SKI3*, *SKI6*, *SKI7*, and *SKI8* block the translation of viral mRNAs (62-64).

In the current study, homologs of most *MAK* and *SKI* genes were identified in *M. restricta*. The results of the transcriptome analysis suggested that most *MAK* genes were downregulated, which may in turn reduce ribosome synthesis in the *M. restricta* strain containing MrV40. In contrast, no *SKI* homolog showed significantly altered transcript levels in the *M. restricta* strain harboring MrV40. Moreover, we found increased expression of genes involved in

388 energy metabolism and programmed cell death in the *M. restricta* strain containing the virus.
389 Overall, our transcriptome analysis revealed that the expression of only a few genes was
390 altered upon virus infection in *M. restricta*. Although the differential expression patterns
391 differed from that of *M. restricta*, *S. cerevisiae* also displayed relatively small changes in
392 fungal host gene expression upon virus infection, possibly because of co-adaptation of the
393 virus within the fungal host (65). Maintenance and propagation of virus within the fungal
394 host may be involved in the post-transcriptional mechanism and may contribute to the
395 minimal changes in host gene expression. Notably, the possibility that an RNA silencing
396 pathway in *M. restricta* cells influences virus maintenance was excluded because of the
397 absence of homologous genes required for the pathway in the genome of the fungus.

398 In addition to transcriptome analysis, we directly investigated whether the virus influences
399 the cellular morphology of *M. restricta* and the structures of its intracellular organelles by
400 TEM. We observed significantly larger vacuoles in virus-infected *M. restricta* cells. An
401 increased vacuole size upon virus infection has been reported previously. The
402 phytopathogenic fungus *Botrytis porri* infected with dsRNA virus 1 showed the formation of
403 abundant vacuoles (66), and turnip mosaic virus induced the large central vacuole in
404 *Nicotiana benthamiana* plant cells (67). Particularly, in *N. benthamiana*, turnip mosaic virus
405 particles were shown to accumulate in vacuoles and be protected by the organelle membranes
406 against the harsh host environment, particularly during xylem vessel differentiation.
407 Furthermore, virus accumulation in vacuoles in plant-to-plant virus transmission has been
408 suggested (67). Although the expression of genes involved in vacuole biogenesis was not
409 altered in transcriptome analysis in *M. restricta* cells containing the virus, there may be a
410 relationship between vacuole functions and MrV40 in *M. restricta*. Therefore, additional

411 physiological studies are needed.

412 TLR3 is well-conserved in most vertebrates, localizes on the endosomal transmembrane, and
413 plays a role in immune and non-immune cells. It has been suggested that TLR3 senses viral
414 dsRNA taken up through endocytosis and contributes to defending the host against viral
415 infection by regulating the expression of a range of cytokines (49, 68). A previous study
416 demonstrated a significant decrease in cytokines (IFN-α/β, IFN-γ, and IL-12p40) and increase
417 in viral PFU in the spleen of *Tlr3*$^{-/-}$ mice infected with mouse cytomegalovirus (69). We
418 found that *TLR3* expression was significantly increased by purified dsRNA from the MrV40
419 particles and cell lysates of *M. restricta* containing the virus. The dsRNA and cell lysates also
420 showed increased production of cytokines involved in inflammation. However, in *Tlr3*$^{-/-}$
421 BMDCs, the production of all cytokines in the cells treated with purified dsRNA from
422 MrV40 and cell lysates of virus containing *M. restricta* was attenuated, suggesting that TLR3
423 plays a central role in the host response against dsRNA of MrV40 and mediates the
424 production of the cytokines. Similarly, the *Leishmania* parasite *L. guyanensis* infected with
425 the dsRNA virus belonging to *Totivirus* induced a TLR3-mediated inflammatory immune
426 response within the vertebrate host, indicating that the *Leishmania* RNA virus (LRV1)
427 functions as an innate immunogen. Moreover, in *Leishmania*, LRV1 was suggested to
428 stimulate the inflammatory immune response and increase the severity and persistence of the
429 parasite (70). However, whether MrV40 causes hyper- or hypo-pathogenesis of *M. restricta*
430 remains unclear. Therefore, further studies to characterize the potential function of MrV40 as
431 an innate immunogen are needed.

432 Overall, our study demonstrated the existence of a dsRNA virus within *M. restricta*. We also
433 determined the sequences and structure of the viral genome along with the independent RNA

segment. Moreover, we identified viruses not only from different strains of *M. restricta* but also from other *Malassezia* species, although variation in the viral genomes was observed. Evidence that the viral nucleic acid from MrV40 induces a TLR3-mediated inflammatory immune response was obtained, suggesting that a viral element contributes to the pathogenesis of *Malassezia*.

Materials and Methods

Strains and growth conditions

Malassezia restricta KCTC 27512, KCTC 27516, KCTC 27518, KCTC 27524, KCTC 27540, KCTC 27543, KCTC 27550, KCTC 27879, KCTC 27880, KCTC 27882, and KCTC 27883, *M. globosa* CBS 7966, *M. pachydermatis* KCTC 27587, and *M. sympodialis* KCTC 27817 were obtained as previously described and cultured on Leeming and Notman agar (LNA) medium at 34°C for 3 days (29, 71-73). Among these strains, *M. restricta* KCTC 27540 was used to identify dsRNA viruses. *Escherichia coli* DH10B and BL21 were grown in Luria-Bertani broth at 37°C.

Purification of virus particles

The virus particles were purified as previously described with some modifications (66). Briefly, approximately 10 g of *M. restricta* cells was harvested and suspended in 10 mL of extraction buffer (0.1 M sodium phosphate buffer containing 3% (v/v) Triton X-100, pH 7.0). The suspended cells were vortexed with glass beads and centrifuged at 10,000 ×*g* at 4°C for 20 min to remove cell debris. The supernatant containing crude extracts was ultracentrifuged

456 at 119,000 ×*g* at 4°C for 2 h to precipitate all particles. The resulting pellet was suspended in
457 1 mL of 0.1 M sodium phosphate buffer (pH 7.0), and the suspension was centrifuged at
458 16,000 ×*g* at 4°C for 30 min to remove large particles. The supernatant was overlaid on
459 sucrose solution with a gradient concentration ranging from 10% to 40% (w/v) and
460 centrifuged at 70,000 ×*g* at 4°C for 2 h. Fractions (700 μL/each fraction) were collected from
461 the top of the ultracentrifuged sucrose gradient solution. Each fraction was analyzed by 1%
462 agarose gel electrophoresis and 8% SDS-PAGE to detect dsRNA segments and protein,
463 respectively. Methods for cell fixation and TEM are described in the Supplementary
464 Materials and Methods.

465

466 **Determination of MrV40L and MrV40S sequences**

467 The reference genome sequence was required to obtain the complete sequence of MrV40L by
468 Illumina Miseq. We first obtained the partial fragment of MrV40L and determined its
469 nucleotide sequence. Briefly, 1 μg of cDNA obtained as described above was amplified using
470 1 μM of the tagged oligo_1 primer to bind the tag and 1.25 units of *Taq* DNA polymerase
471 (BIONEER, Daejeon, Korea). The amplicons were cloned into the pGEM-T vector (Promega,
472 Madison, WI, USA), transformed into *E. coli* DH10B, and sequenced with the universal M13
473 primers. The resulting partial sequences of MrV40L showed high similarity with the genome
474 of *Scheffersomyces segobiensis* virus L isolate NRRL Y-11571, which was used to assemble
475 the reference genome in our study. To sequence the entire genome of the virus from *M.*
476 *restricta* KCTC 27540, dsRNA was purified using Cellulose A (Advantec, Taipei, Taiwan)
477 from total cell extract as described previously (74). After purification, purified dsRNA was
478 treated with Ambion™ DNase I (Thermo Fisher Scientific, Waltham, MA, USA) to remove

479 remaining genomic DNA remained. The sequencing library was constructed using the TruSeq
480 Stranded Total RNA Sample Prep Kit (Illumina, San Diego, CA, USA) following the
481 manufacturer's instructions and excluding poly-A selection. The resulting library was
482 sequenced on an Illumina MiSeq instrument according to the manufacturer's instructions.
483 The generated raw sequences, 250-bp paired-end reads, were assembled by CLC Genomics
484 Workbench v7.5 (Qiagen, Hilden, Germany), and the resulting contigs were identified by
485 BLASTN of the NCBI nucleotide database. Based on the reference genome, two contigs of
486 MrV40L were assembled. The gap between the contigs was sequenced by gap-filling RT-PCR
487 using primers Linkage1_V40 and Linkage2_V40) (see Table S2), and both termini were
488 sequenced by RACE PCR using a 5′/3′ RACE Kit, 2nd Generation (Roche, Basel, Switzerland)
489 according to the 5′ RACE protocol described by the manufacturer.

490 To determine the MrV40S genome, the RACE PCR method was used because we failed to
491 find any contig of MrV40S. Like MrV40L, the partial sequence of cDNA from MrV40S was
492 amplified using the tagged oligo_1 primer. The amplicons were cloned into the pGEM-T
493 vector (Promega) and sequenced. Using the partial sequence obtained, 5′ RACE PCR was
494 performed and repeated until no additional sequence was found.

495

496 ***In silico* analysis**

497 To identify the ORFs in MrV40L and MrV40S, the nucleotide sequences of the genomes
498 were analyzed by ORFfinder (https://www.ncbi.nlm.nih.gov/orffinder/). To predict ribosomal
499 frameshift signals, a putative slippery site was identified using FSFinder2 (75). The amino
500 acid sequences of CP and RDRP of MrV40L were analyzed using the Pfam database
501 (http://pfam.xfam.org/) and BLASTP (https://blast.ncbi.nlm.nih.gov/). For sequence

alignment, Jalview2.0 was used (76). The phylogenetic tree showing the relationship of MrV40L with RDRP of other dsRNA fungal viruses was constructed using MEGA X, and phylogenetic reconstruction analysis was performed by the neighbor-joining method with 1,000 bootstrap replications (77, 78).

Mice and cell culture

Wild-type C57BL/6 mice were purchased from Orient Bio Co. (Gyeonggi-do, Korea). *TLR3*$^{-/-}$ (B6;129S1-Tlr3^{tm1Flv}/J, 005217) mice were obtained from Jackson Laboratory (Bar Harbor, ME, USA). All animal experimental procedures were reviewed and approved by the Institutional Animal Care and Use Committee of Hanyang University (protocol 2018-0085) and performed in accordance with Korean Food and Drug Administration guidelines. All animals were maintained in a specific pathogen-free environment. Primary BMDCs were isolated from C57BL/6 mice and cultured in Dulbecco's modified Eagle medium for 3–5 days in the presence of 20 ng/mL recombinant granulocyte-macrophage colony-stimulating factor (R&D Systems, Minneapolis, MN, USA) as described previously (79). Cell cultures were stained to detect dendritic cells with CD11c-FITC (eBiosciences, San Diego, CA, USA).

Cytokine measurement

Mouse cytokines in the culture supernatants were measured with a BD OptEIA ELISA set (BD Biosciences, Franklin Lakes, NJ, USA) as described previously (80). All assays were performed according to the manufacturer's instructions. Phosphate-buffered saline (PBS) and lipopolysaccharide served as a negative and positive controls, respectively.

524

525 **cDNA synthesis, RNA isolation, transcriptome analysis, quantitative real-time PCR, and**
526 **heterologous expression and purification of MrV40 proteins**

527 See Supplementary Materials and Methods

528

529 **Data availability**

530 The complete genome sequences of MrV40L and MrV40S were deposited into Genbank
531 under accession numbers MN603497 and MN603498, respectively. The transcriptome data
532 was deposited in Gene Express Omnibus under the accession number GSE138985.

533

534 **Acknowledgments**

535 We thank James W. Kronstad for critical reading of the manuscript. There is a companion
536 paper from the Joe Heitman group at Duke University, and we thank Joe Heitman and
537 Giuseppe Ianiri for communication. This work was supported by the National Research
538 Foundation of Korea (NRF) grant funded by the Korea government (MSIT)
539 2019R1A4A1024764 (WHJ), and 2019R1I1A2A01064237 (CSY).

540

541

542

References

1. Hollings M. 1962. Viruses associated with a die-back disease of cultivated mushroom. Nature 196:962.

2. Ghabrial SA, Caston JR, Jiang D, Nibert ML, Suzuki N. 2015. 50-plus years of fungal viruses. Virology 479-480:356-68.

3. Bussey H. 1991. K1 killer toxin, a pore-forming protein from yeast. Mol Microbiol 5:2339-43.

4. Hannig EM, Leibowitz MJ. 1985. Structure and expression of the M2 genomic segment of a type 2 killer virus of yeast. Nucleic Acids Res 13:4379-400.

5. Schmitt MJ, Tipper DJ. 1990. K28, a unique double-stranded RNA killer virus of Saccharomyces cerevisiae. Mol Cell Biol 10:4807-15.

6. Rodriguez-Cousino N, Maqueda M, Ambrona J, Zamora E, Esteban R, Ramirez M. 2011. A new wine Saccharomyces cerevisiae killer toxin (Klus), encoded by a double-stranded rna virus, with broad antifungal activity is evolutionarily related to a chromosomal host gene. Appl Environ Microbiol 77:1822-32.

7. Cheng RH, Caston JR, Wang G-j, Gu F, Smith TJ, Baker TS, Bozarth RF, Trus BL, Cheng N, Wickner RB. 1994. Fungal virus capsids, cytoplasmic compartments for the replication of double-stranded RNA, formed as icosahedral shells of asymmetric Gag dimers. Elsevier.

8. Icho T, Wickner RB. 1989. The double-stranded RNA genome of yeast virus L-A encodes its own putative RNA polymerase by fusing two open reading frames. J Biol Chem

264:6716-23.

9. Hopper JE, Bostian K, Rowe L, Tipper D. 1977. Translation of the L-species dsRNA genome of the killer-associated virus-like particles of Saccharomyces cerevisiae. Journal of Biological Chemistry 252:9010-9017.

10. Fujimura T, Wickner RB. 1988. Gene overlap results in a viral protein having an RNA binding domain and a major coat protein domain. Cell 55:663-671.

11. Dinman JD, Icho T, Wickner RB. 1991. A -1 ribosomal frameshift in a double-stranded RNA virus of yeast forms a gag-pol fusion protein. Proc Natl Acad Sci U S A 88:174-8.

12. Van Alfen NK, Jaynes RA, Anagnostakis SL, Day PR. 1975. Chestnut Blight: Biological Control by Transmissible Hypovirulence in Endothia parasitica. Science 189:890-1.

13. Choi GH, Nuss DL. 1992. Hypovirulence of chestnut blight fungus conferred by an infectious viral cDNA. Science 257:800-3.

14. Ghabrial SA, Suzuki N. 2009. Viruses of plant pathogenic fungi. Annu Rev Phytopathol 47:353-84.

15. Segers GC, Zhang X, Deng F, Sun Q, Nuss DL. 2007. Evidence that RNA silencing functions as an antiviral defense mechanism in fungi. Proc Natl Acad Sci U S A 104:12902-6.

16. Zhang X, Segers GC, Sun Q, Deng F, Nuss DL. 2008. Characterization of hypovirus-derived small RNAs generated in the chestnut blight fungus by an inducible DCL-2-dependent pathway. J Virol 82:2613-9.

585 17. Hammond TM, Andrewski MD, Roossinck MJ, Keller NP. 2008. Aspergillus
586 mycoviruses are targets and suppressors of RNA silencing. Eukaryot Cell 7:350-7.

587 18. Yaegashi H, Shimizu T, Ito T, Kanematsu S. 2016. Differential Inductions of RNA
588 Silencing among Encapsidated Double-Stranded RNA Mycoviruses in the White Root Rot
589 Fungus Rosellinia necatrix. J Virol 90:5677-92.

590 19. Yu J, Lee KM, Cho WK, Park JY, Kim KH. 2018. Differential Contribution of RNA
591 Interference Components in Response to Distinct Fusarium graminearum Virus Infections. J
592 Virol 92.

593 20. Findley K, Oh J, Yang J, Conlan S, Deming C, Meyer JA, Schoenfeld D, Nomicos E,
594 Park M, Program NIHISCCS, Kong HH, Segre JA. 2013. Topographic diversity of fungal
595 and bacterial communities in human skin. Nature 498:367-70.

596 21. Clavaud C, Jourdain R, Bar-Hen A, Tichit M, Bouchier C, Pouradier F, El Rawadi C,
597 Guillot J, Ménard-Szczebara F, Breton L. 2013. Dandruff is associated with disequilibrium in
598 the proportion of the major bacterial and fungal populations colonizing the scalp. PloS one
599 8:e58203.

600 22. Patino-Uzcategui A, Amado Y, Cepero de Garcia M, Chaves D, Tabima J, Motta A,
601 Cardenas M, Bernal A, Restrepo S, Celis A. 2011. Virulence gene expression in Malassezia
602 spp from individuals with seborrheic dermatitis. J Invest Dermatol 131:2134-6.

603 23. Zhang E, Tanaka T, Tajima M, Tsuboi R, Nishikawa A, Sugita T. 2011.
604 Characterization of the skin fungal microbiota in patients with atopic dermatitis and in
605 healthy subjects. Microbiol Immunol 55:625-32.

606 24. Park T, Kim HJ, Myeong NR, Lee HG, Kwack I, Lee J, Kim BJ, Sul WJ, An S. 2017.

607 Collapse of human scalp microbiome network in dandruff and seborrhoeic dermatitis.
608 Experimental dermatology 26:835-838.

609 25. Wang L, Clavaud C, Bar-Hen A, Cui M, Gao J, Liu Y, Liu C, Shibagaki N, Guéniche
610 A, Jourdain R. 2015. Characterization of the major bacterial–fungal populations colonizing
611 dandruff scalps in Shanghai, China, shows microbial disequilibrium. Experimental
612 dermatology 24:398-400.

613 26. Xu Z, Wang Z, Yuan C, Liu X, Yang F, Wang T, Wang J, Manabe K, Qin O, Wang X.
614 2016. Dandruff is associated with the conjoined interactions between host and
615 microorganisms. Scientific reports 6:srep24877.

616 27. Grice EA, Dawson TL, Jr. 2017. Host-microbe interactions: Malassezia and human
617 skin. Curr Opin Microbiol 40:81-87.

618 28. Sharma S, Gupta S, Shrivastava JN. 2011. Presence of Virus like Particles in Human
619 Pathogenic Fungi: Chrysosporium sps and Candida albicans. Indian J Virol 22:104-10.

620 29. Park M, Cho YJ, Lee YW, Jung WH. 2017. Whole genome sequencing analysis of
621 the cutaneous pathogenic yeast Malassezia restricta and identification of the major lipase
622 expressed on the scalp of patients with dandruff. Mycoses 60:188-197.

623 30. EDY VG, SZEKELY M, LOVINY T, DREYER C. 1976. Action of Nucleases on
624 Double-Stranded RNA. European journal of biochemistry 61:563-572.

625 31. Sommer SS, Wickner RB. 1982. Yeast L dsRNA consists of at least three distinct
626 RNAs; evidence that the non-Mendelian genes [HOK],[NEX] and [EXL] are on one of these
627 dsRNAs. Cell 31:429-441.

628 32. Park CM, Lopinski JD, Masuda J, Tzeng TH, Bruenn JA. 1996. A second double-
629 stranded RNA virus from yeast. Virology 216:451-4.

630 33. Taylor DJ, Ballinger MJ, Bowman SM, Bruenn JA. 2013. Virus-host co-evolution
631 under a modified nuclear genetic code. PeerJ 1:e50.

632 34. Bruenn JA. 1993. A closely related group of RNA-dependent RNA polymerases from
633 double-stranded RNA viruses. Nucleic Acids Res 21:5667-9.

634 35. Schmitt MJ, Breinig F. 2002. The viral killer system in yeast: from molecular biology
635 to application. FEMS microbiology reviews 26:257-276.

636 36. Wickner RB, Leibowitz MJ. 1979. Mak mutants of yeast: mapping and
637 characterization. J Bacteriol 140:154-60.

638 37. Tercero J, Dinman J, Wickner R. 1993. Yeast MAK3 N-acetyltransferase recognizes
639 the N-terminal four amino acids of the major coat protein (gag) of the LA double-stranded
640 RNA virus. Journal of bacteriology 175:3192-3194.

641 38. Tercero J, Wickner RB. 1992. MAK3 encodes an N-acetyltransferase whose
642 modification of the LA gag NH2 terminus is necessary for virus particle assembly. Journal of
643 Biological Chemistry 267:20277-20281.

644 39. Fujimura T, Wickner RB. 1987. LA double-stranded RNA viruslike particle
645 replication cycle in Saccharomyces cerevisiae: particle maturation in vitro and effects of
646 mak10 and pet18 mutations. Molecular and cellular biology 7:420-426.

647 40. Lee Y-J, Wickner R. 1992. MAK10, a glucose-repressible gene necessary for
648 replication of a dsRNA virus of Saccharomyces cerevisiae, has T cell receptor alpha-subunit

649 motifs. Genetics 132:87-96.

650 41. Wickner RB, Ridley SP, Fried HM, Ball SG. 1982. Ribosomal protein L3 is involved
651 in replication or maintenance of the killer double-stranded RNA genome of Saccharomyces
652 cerevisiae. Proceedings of the National Academy of Sciences 79:4706-4708.

653 42. Ohtake Y, Wickner RB. 1995. Yeast virus propagation depends critically on free 60S
654 ribosomal subunit concentration. Molecular and Cellular Biology 15:2772-2781.

655 43. Ryu S-W, Lee S-J, Park M-Y, Jun J-i, Jung Y-K, Kim E. 2003. Fas-associated factor 1,
656 FAF1, is a member of Fas death-inducing signaling complex. Journal of Biological Chemistry
657 278:24003-24010.

658 44. Fujikura D, Miyazaki T. 2018. Programmed Cell Death in the Pathogenesis of
659 Influenza. Int J Mol Sci 19.

660 45. Jorgensen I, Rayamajhi M, Miao EA. 2017. Programmed cell death as a defence
661 against infection. Nat Rev Immunol 17:151-164.

662 46. Banks GT, Buck KW, Chain EB, Himmelweit F, Marks JE, Tyler JM, Hollings M,
663 Last FT, Stone OM. 1968. Viruses in fungi and interferon stimulation. Nature 218:542-5.

664 47. Kleinschmidt WJ, Cline JC, Murphy EB. 1964. Interferon Production Induced by
665 Statolon. Proc Natl Acad Sci U S A 52:741-4.

666 48. Lampson GP, Tytell AA, Field AK, Nemes MM, Hilleman MR. 1967. Inducers of
667 interferon and host resistance. I. Double-stranded RNA from extracts of Penicillium
668 funiculosum. Proc Natl Acad Sci U S A 58:782-9.

669 49. Perales-Linares R, Navas-Martin S. 2013. Toll-like receptor 3 in viral pathogenesis:

670 friend or foe? Immunology 140:153-67.

671 50. Thompson MR, Kaminski JJ, Kurt-Jones EA, Fitzgerald KA. 2011. Pattern
672 recognition receptors and the innate immune response to viral infection. Viruses 3:920-40.

673 51. Claudepierre MC, Hortelano J, Schaedler E, Kleinpeter P, Geist M, Remy-Ziller C,
674 Brandely R, Tosch C, Laruelle L, Jawhari A, Menguy T, Marchand JB, Romby P, Schultz P,
675 Hartmann G, Rooke R, Bonnefoy JY, Preville X, Rittner K. 2014. Yeast virus-derived
676 stimulator of the innate immune system augments the efficacy of virus vector-based
677 immunotherapy. J Virol 88:5242-55.

678 52. Ishikawa T, Itoh F, Yoshida S, Saijo S, Matsuzawa T, Gonoi T, Saito T, Okawa Y,
679 Shibata N, Miyamoto T, Yamasaki S. 2013. Identification of distinct ligands for the C-type
680 lectin receptors Mincle and Dectin-2 in the pathogenic fungus Malassezia. Cell Host Microbe
681 13:477-88.

682 53. Vargas G, Rocha JD, Oliveira DL, Albuquerque PC, Frases S, Santos SS, Nosanchuk
683 JD, Gomes AM, Medeiros LC, Miranda K, Sobreira TJ, Nakayasu ES, Arigi EA, Casadevall
684 A, Guimaraes AJ, Rodrigues ML, Freire-de-Lima CG, Almeida IC, Nimrichter L. 2015.
685 Compositional and immunobiological analyses of extracellular vesicles released by Candida
686 albicans. Cell Microbiol 17:389-407.

687 54. Samuel CE. 2001. Antiviral actions of interferons. Clinical microbiology reviews
688 14:778-809.

689 55. Brierley I, Boursnell ME, Binns MM, Bilimoria B, Blok VC, Brown TD, Inglis SC.
690 1987. An efficient ribosomal frame-shifting signal in the polymerase-encoding region of the
691 coronavirus IBV. EMBO J 6:3779-85.

692 56. Jacks T, Varmus HE. 1985. Expression of the Rous sarcoma virus pol gene by
693 ribosomal frameshifting. Science 230:1237-42.

694 57. Jacks T, Madhani HD, Masiarz FR, Varmus HE. 1988. Signals for ribosomal
695 frameshifting in the Rous sarcoma virus gag-pol region. Cell 55:447-58.

696 58. Magliani W, Conti S, Gerloni M, Bertolotti D, Polonelli L. 1997. Yeast killer systems.
697 Clinical microbiology reviews 10:369-400.

698 59. Tercero JC, Riles LE, Wickner RB. 1992. Localized mutagenesis and evidence for
699 post-transcriptional regulation of MAK3. A putative N-acetyltransferase required for double-
700 stranded RNA virus propagation in Saccharomyces cerevisiae. J Biol Chem 267:20270-6.

701 60. Wickner RB. 1996. Double-stranded RNA viruses of Saccharomyces cerevisiae.
702 Microbiological reviews 60:250.

703 61. Thrash C, Bankier AT, Barrell BG, Sternglanz R. 1985. Cloning, characterization,
704 and sequence of the yeast DNA topoisomerase I gene. Proceedings of the National Academy
705 of Sciences 82:4374-4378.

706 62. Widner WR, Wickner RB. 1993. Evidence that the SKI antiviral system of
707 Saccharomyces cerevisiae acts by blocking expression of viral mRNA. Molecular and
708 cellular biology 13:4331-4341.

709 63. Masison DC, Blanc A, Ribas JC, Carroll K, Sonenberg N, Wickner RB. 1995.
710 Decoying the cap-mRNA degradation system by a double-stranded RNA virus and poly (A)-
711 mRNA surveillance by a yeast antiviral system. Molecular and Cellular Biology 15:2763-
712 2771.

713 64. Benard L, Carroll K, Valle RC, Masison DC, Wickner RB. 1999. The ski7 antiviral
714 protein is an EF1-α homolog that blocks expression of non-Poly (A) mRNA in
715 Saccharomyces cerevisiae. Journal of virology 73:2893-2900.

716 65. McBride RC, Boucher N, Park DS, Turner PE, Townsend JP. 2013. Yeast response to
717 LA virus indicates coadapted global gene expression during mycoviral infection. FEMS yeast
718 research 13:162-179.

719 66. Wu M, Jin F, Zhang J, Yang L, Jiang D, Li G. 2012. Characterization of a novel
720 bipartite double-stranded RNA mycovirus conferring hypovirulence in the phytopathogenic
721 fungus Botrytis porri. J Virol 86:6605-19.

722 67. Wan J, Basu K, Mui J, Vali H, Zheng H, Laliberte JF. 2015. Ultrastructural
723 Characterization of Turnip Mosaic Virus-Induced Cellular Rearrangements Reveals
724 Membrane-Bound Viral Particles Accumulating in Vacuoles. J Virol 89:12441-56.

725 68. Matsumoto M, Oshiumi H, Seya T. 2011. Antiviral responses induced by the TLR3
726 pathway. Reviews in Medical Virology 21:67-77.

727 69. Tabeta K, Georgel P, Janssen E, Du X, Hoebe K, Crozat K, Mudd S, Shamel L,
728 Sovath S, Goode J. 2004. Toll-like receptors 9 and 3 as essential components of innate
729 immune defense against mouse cytomegalovirus infection. Proceedings of the National
730 Academy of Sciences 101:3516-3521.

731 70. Hartley MA, Ronet C, Zangger H, Beverley SM, Fasel N. 2012. Leishmania RNA
732 virus: when the host pays the toll. Frontiers in Cellular and Infection Microbiology 2.

733 71. Kim M, Cho Y-J, Park M, Choi Y, Hwang SY, Jung WH. 2018. Genomic tandem
734 quadruplication is associated with ketoconazole resistance in Malassezia pachydermatis. J

735 Microbiol Biotechnol 28:1937-1945.

736 72. Park M, Jung WH, Han SH, Lee YH, Lee YW. 2015. Characterisation and
737 Expression Analysis of MrLip1, a Class 3 Family Lipase of Malassezia restricta. Mycoses
738 58:671-8.

739 73. Leeming JP, Notman FH. 1987. Improved methods for isolation and enumeration of
740 Malassezia furfur from human skin. J Clin Microbiol 25:2017-9.

741 74. Okada R, Kiyota E, Moriyama H, Fukuhara T, Natsuaki T. 2015. A simple and rapid
742 method to purify viral dsRNA from plant and fungal tissue. Journal of General Plant
743 Pathology 81:103-107.

744 75. Moon S, Byun Y, Kim HJ, Jeong S, Han K. 2004. Predicting genes expressed via -1
745 and +1 frameshifts. Nucleic Acids Res 32:4884-92.

746 76. Waterhouse AM, Procter JB, Martin DM, Clamp M, Barton GJ. 2009. Jalview
747 Version 2--a multiple sequence alignment editor and analysis workbench. Bioinformatics
748 25:1189-91.

749 77. Kumar S, Nei M, Dudley J, Tamura K. 2008. MEGA: a biologist-centric software for
750 evolutionary analysis of DNA and protein sequences. Brief Bioinform 9:299-306.

751 78. Kumar S, Stecher G, Li M, Knyaz C, Tamura K. 2018. MEGA X: Molecular
752 Evolutionary Genetics Analysis across Computing Platforms. Mol Biol Evol 35:1547-1549.

753 79. Vargas G, Rocha JD, Oliveira DL, Albuquerque PC, Frases S, Santos SS, Nosanchuk
754 JD, Gomes AMO, Medeiros LC, Miranda K. 2015. Compositional and immunobiological
755 analyses of extracellular vesicles released by C andida albicans. Cellular microbiology

17:389-407.

80. Koh H-J, Kim Y-R, Kim J-S, Yun J-S, Kim S, Kim SY, Jang K, Yang C-S. 2018. CD82 hypomethylation is essential for tuberculosis pathogenesis via regulation of RUNX1-Rab5/22. Experimental & molecular medicine 50:62.

81. Saitou N, Nei M. 1987. The neighbor-joining method: a new method for reconstructing phylogenetic trees. Mol Biol Evol 4:406-25.

82. Felsenstein J. 1985. Confidence Limits on Phylogenies: An Approach Using the Bootstrap. Evolution 39:783-791.

83. Sanderlin RS, Ghabrial SA. 1978. Physicochemical properties of two distinct types of virus-like particles from Helminthosporium victoriae. Virology 87:142-51.

84. Shapira R, Choi GH, Nuss DL. 1991. Virus-like genetic organization and expression strategy for a double-stranded RNA genetic element associated with biological control of chestnut blight. EMBO J 10:731-9.

85. Hillman BI, Halpern BT, Brown MP. 1994. A viral dsRNA element of the chestnut blight fungus with a distinct genetic organization. Virology 201:241-50.

86. Van der Lende TR, Duitman EH, Gunnewijk MG, Yu L, Wessels JG. 1996. Functional analysis of dsRNAs (L1, L3, L5, and M2) associated with isometric 34-nm virions of Agaricus bisporus (white button mushroom). Virology 217:88-96.

87. Nomura K, Osaki H, Iwanami T, Matsumoto N, Ohtsu Y. 2003. Cloning and characterization of a totivirus double-stranded RNA from the plant pathogenic fungus, Helicobasidium mompa Tanaka. Virus Genes 26:219-26.

777 88. Tuomivirta TT, Hantula J. 2003. Two unrelated double-stranded RNA molecule
778 patterns in Gremmeniella abietina type A code for putative viruses of the families Totiviridae
779 and Partitiviridae. Arch Virol 148:2293-305.

780 89. Jiang D, Ghabrial SA. 2004. Molecular characterization of Penicillium chrysogenum
781 virus: reconsideration of the taxonomy of the genus Chrysovirus. J Gen Virol 85:2111-21.

782 90. Urayama S, Ohta T, Onozuka N, Sakoda H, Fukuhara T, Arie T, Teraoka T,
783 Moriyama H. 2012. Characterization of Magnaporthe oryzae chrysovirus 1 structural proteins
784 and their expression in Saccharomyces cerevisiae. J Virol 86:8287-95.

785 91. Wu Q, Luo Y, Lu R, Lau N, Lai EC, Li WX, Ding SW. 2010. Virus discovery by
786 deep sequencing and assembly of virus-derived small silencing RNAs. Proc Natl Acad Sci U
787 S A 107:1606-11.

788 92. Isawa H, Kuwata R, Hoshino K, Tsuda Y, Sakai K, Watanabe S, Nishimura M, Satho
789 T, Kataoka M, Nagata N, Hasegawa H, Bando H, Yano K, Sasaki T, Kobayashi M, Mizutani
790 T, Sawabe K. 2011. Identification and molecular characterization of a new nonsegmented
791 double-stranded RNA virus isolated from Culex mosquitoes in Japan. Virus Res 155:147-55.

792 93. Mor SK, Phelps NB. 2016. Molecular detection of a novel totivirus from golden
793 shiner (Notemigonus crysoleucas) baitfish in the USA. Arch Virol 161:2227-34.

794 94. Yang X, Zhang Y, Ge X, Yuan J, Shi Z. 2012. A novel totivirus-like virus isolated
795 from bat guano. Arch Virol 157:1093-9.

796 95. Zhai Y, Attoui H, Mohd Jaafar F, Wang HQ, Cao YX, Fan SP, Sun YX, Liu LD,
797 Mertens PP, Meng WS, Wang D, Liang G. 2010. Isolation and full-length sequence analysis
798 of Armigeres subalbatus totivirus, the first totivirus isolate from mosquitoes representing a

799 proposed novel genus (Artivirus) of the family Totiviridae. J Gen Virol 91:2836-45.

800 96. Dihanich M, Van Tuinen E, Lambris J, Marshallsay B. 1989. Accumulation of
801 viruslike particles in a yeast mutant lacking a mitochondrial pore protein. Molecular and
802 cellular biology 9:1100-1108.

803 97. Leibowitz MJ, Wickner RB. 1978. pet 18: A chromosomal gene required for cell
804 growth and for the maintenance of mitochondrial DNA and the killer plasmid of yeast.
805 Molecular and General Genetics MGG 165:115-121.

806 98. Toh-e A, Sahashi Y. 1985. The PET18 locus of Saccharomyces cerevisiae: a complex
807 locus containing multiple genes. Yeast 1:159-171.

808 99. Thrash C, Voelkel K, DiNardo S, Sternglanz R. 1984. Identification of
809 Saccharomyces cerevisiae mutants deficient in DNA topoisomerase I activity. Journal of
810 Biological Chemistry 259:1375-1377.

811 100. Icho T, Wickner RB. 1988. The MAK11 protein is essential for cell growth and
812 replication of M double-stranded RNA and is apparently a membrane-associated protein.
813 Journal of Biological Chemistry 263:1467-1475.

814 101. Wickner RB. 1988. Host function of MAK16: G1 arrest by a mak16 mutant of
815 Saccharomyces cerevisiae. Proceedings of the National Academy of Sciences 85:6007-6011.

816 102. Carroll K, Wickner RB. 1995. Translation and M1 double-stranded RNA propagation:
817 MAK18= RPL41B and cycloheximide curing. Journal of bacteriology 177:2887-2891.

818 103. Toh-E A, Guerry P, Wickner RB. 1978. Chromosomal superkiller mutants of
819 Saccharomyces cerevisiae. Journal of bacteriology 136:1002-1007.

820 104. Ball SG, Tirtiaux C, Wickner RB. 1984. Genetic control of LA and L-(BC) dsRNA
821 copy number in killer systems of Saccharomyces cerevisiae. Genetics 107:199-217.

822 105. Ridley SP, Sommer SS, Wickner RB. 1984. Superkiller mutations in Saccharomyces
823 cerevisiae suppress exclusion of M2 double-stranded RNA by LA-HN and confer cold
824 sensitivity in the presence of M and LA-HN. Molecular and Cellular Biology 4:761-770.

825 106. Dmochowska A, Dignard D, Henning D, Thomas DY, Bussey H. 1987. Yeast KEX1
826 gene encodes a putative protease with a carboxypeptidase B-like function involved in killer
827 toxin and α-factor precursor processing. Cell 50:573-584.

828 107. Wickner RB. 1974. Chromosomal and nonchromosomal mutations affecting the"
829 killer character" of Saccharomyces cerevisiae. Genetics 76:423-432.

830 108. Wickner RB, Leibowitz MJ. 1976. Two chromosomal genes required for killing
831 expression in killer strains of Saccharomyces cerevisiae. Genetics 82:429-442.

832

833

834 **Table 1. The number of differentially expressed genes regulated by virus**

	The number of differential expressed genes (+virus/-virus)				
	2-fold	3-fold	4-fold	>5-fold	Total
Upregulated	204	32	12	10	258
Downregulated	597	152	70	60	809

835

836

837

838

839 **Table 2. Differential expression of genes involved in maintaining dsRNA virus**

S. cerevisiae gene	An encoded protein and/or function	Needed by *S. cerevisiae* virus	*M. restricta* gene ID	Fold change (+virus/−virus)	Reference(s)
MAK3	N-acetyltransferase modifying Gag	L-A, M	MRET_0174	0.62	(38, 59)
MAK10	Non-catalytic subunit of N-terminal acetyltransferase		No hits		(40, 96)
PET18 (MAK30+MAK31)	Unknown		No hits		(97, 98)
MAK1 (TOP1)	DNA topoisomerase I	M	MRET_0706	0.41	(99)
MAK2	60S subunit biosynthesis		MRET_4192	0.88	(42)
MAK5			MRET_0265	0.44	
MAK21			MRET_2922	0.24	
MAK11			MRET_2252	0.40	(42, 100)
MAK16			MRET_2745	0.48	(42, 101)
MAK7 (*RPL4A*)	60S subunit protein L4		No hits		(42)
MAK8 (*TCM1*)	60S subunit protein L3		MRET_1592	0.24	(41)
MAK18 (*RPL41B*)	60S subunit protein L41		MRET_2856	0.60	(102)

SKI1 (*XRN1*)	5′-3′ exonuclease		MRET_4129	0.73	(103)
SKI2	RNA helicase		MRET_2647	0.91	(104, 105)
SKI3	Tetratricopeptide repeat protein		MRET_1481	0.78	
SKI4 (*CSL4*)	Exosome non-catalytic core component	L-A, M	MRET_2576	0.96	
SKI6	Exosome non-catalytic core component		MRET_3188	0.55	
SKI7	GTP-binding protein		No hits		
SKI8	WD-repeat protein		No hits		
KEX1	Cell death protease essential for hypochlorite-induced apoptosis	M	MRET_4176	0.93	(106-108)
KEX2	Kexin, a subtilisin-like protease (proprotein convertase)		MRET_0618	1.13	(107, 108)

840

841

842

843 **Table 3. Differential expression of genes involved in TCA cycle and electron transport chain**

Gene	Annotation	Fold change (+virus/−virus)
MRET_1104	NADH dehydrogenase (ubiquinone) Fe-S protein 7	2.85
MRET_1378	succinate dehydrogenase (ubiquinone) iron-sulfur subunit	3.55
MRET_1709	cytochrome c	2.56
MRET_1953	NADH dehydrogenase (ubiquinone) Fe-S protein 1	2.44
MRET_2042	fumarate hydratase, class II	2.42
MRET_2097	succinate dehydrogenase (ubiquinone) flavoprotein subunit	2.19
MRET_2956	2-oxoglutarate dehydrogenase E1 component	2.21
MRET_3173	dihydrolipoamide dehydrogenase	2.27
MRET_4117	aconitate hydratase	3.55

844

845

846

847 **Figures**

848

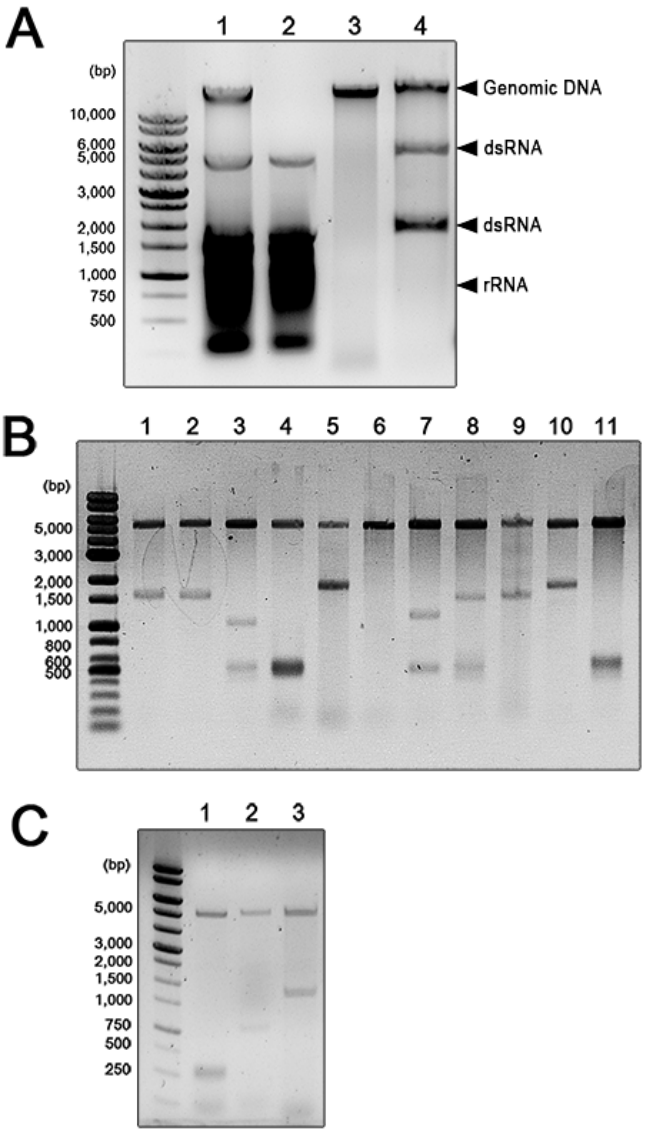

849

850 **Fig. 1. Extrachromosomal dsRNA segments in *Malassezia*.** (A) Nucleic acids from *M.*
851 *restricta* KCTC 27540 were separated on a 0.7% agarose gel. Lane 1, total nucleic acids; lane
852 2, total nucleic acids treated with DNase I; lane 3, total nucleic acids treated with RNase A;
853 lane 4, total nucleic acids treated with RNase T1. (B) Presence of dsRNA in *M. restricta*

strains. The dsRNAs in *M. restricta* strains were separated on a 0.7% agarose gel. Each lane indicates *M. restricta* strains in which dsRNAs were found as follows: lane 1, *M. restricta* KCTC 27540; lane 2, *M. restricta* KCTC 27512; lane 3, *M. restricta* KCTC 27516; lane 4, *M. restricta* KCTC 27518; lane 5, *M. restricta* KCTC 27524; lane 6, *M. restricta* KCTC 27543; lane 7, *M. restricta* KCTC 27550; lane 8, *M. restricta* KCTC 27879; lane 9, *M. restricta* KCTC 27880; lane 10, *M. restricta* KCTC 27882; lane 11, *M. restricta* KCTC 27883. (C) dsRNAs were extracted from different *Malassezia* species and separated on a 0.7% agarose gel. Lane 1, *M. globosa* CBS 7966; lane 2, *M. pachydermatis* KCTC 27587; lane 3, *M. sympodialis* KCTC 27817.

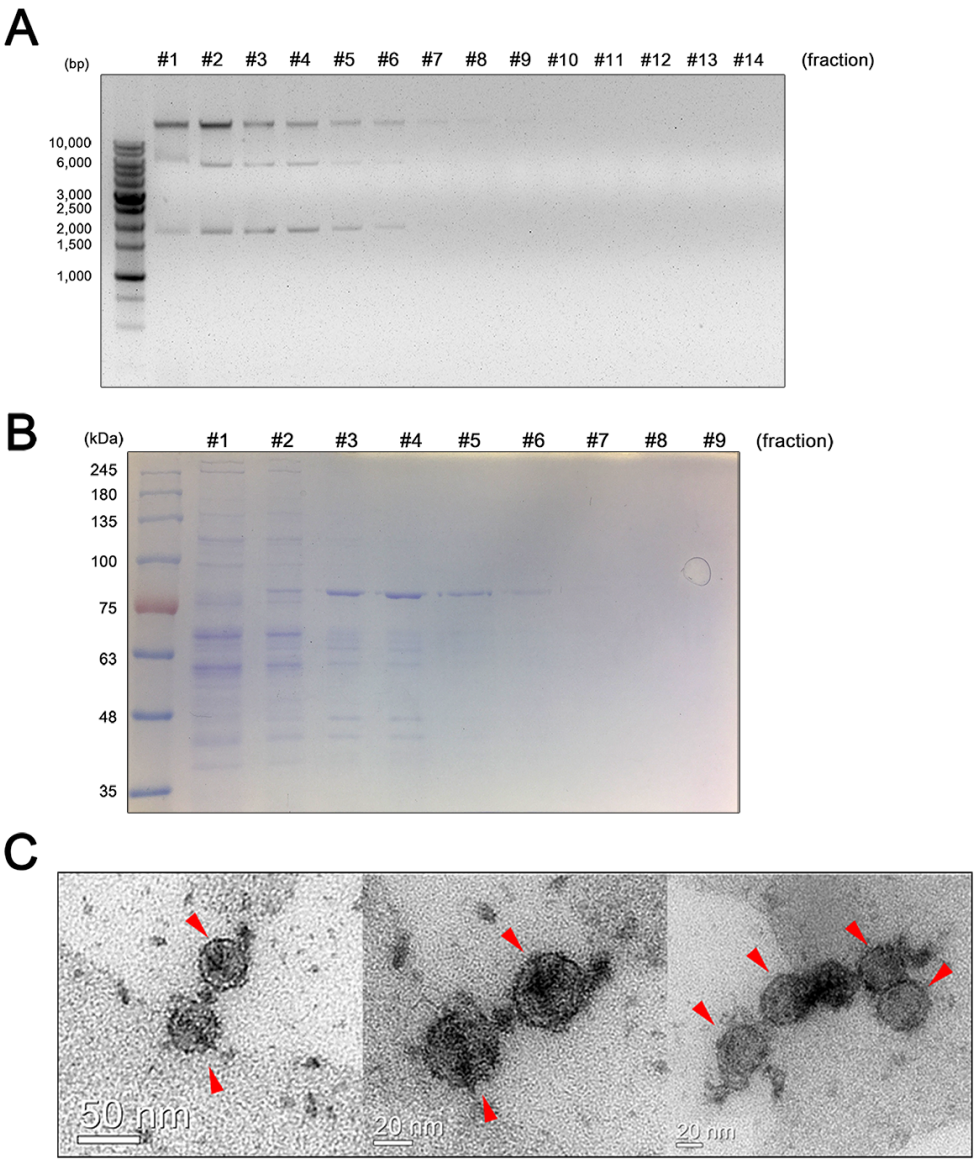

866

867 **Fig. 2. Isolation of virus particles from *M. restricta* KCTC 27540, and their TEM images.**

868 The collected fractions after sucrose gradient ultracentrifugation were analyzed for their

869 nucleic acids and proteins on an agarose gel (A) and SDS-PAGE gel (B), respectively. Images

870 of the viral particles (red arrows) were obtained using a transmission electron microscope (C).

871

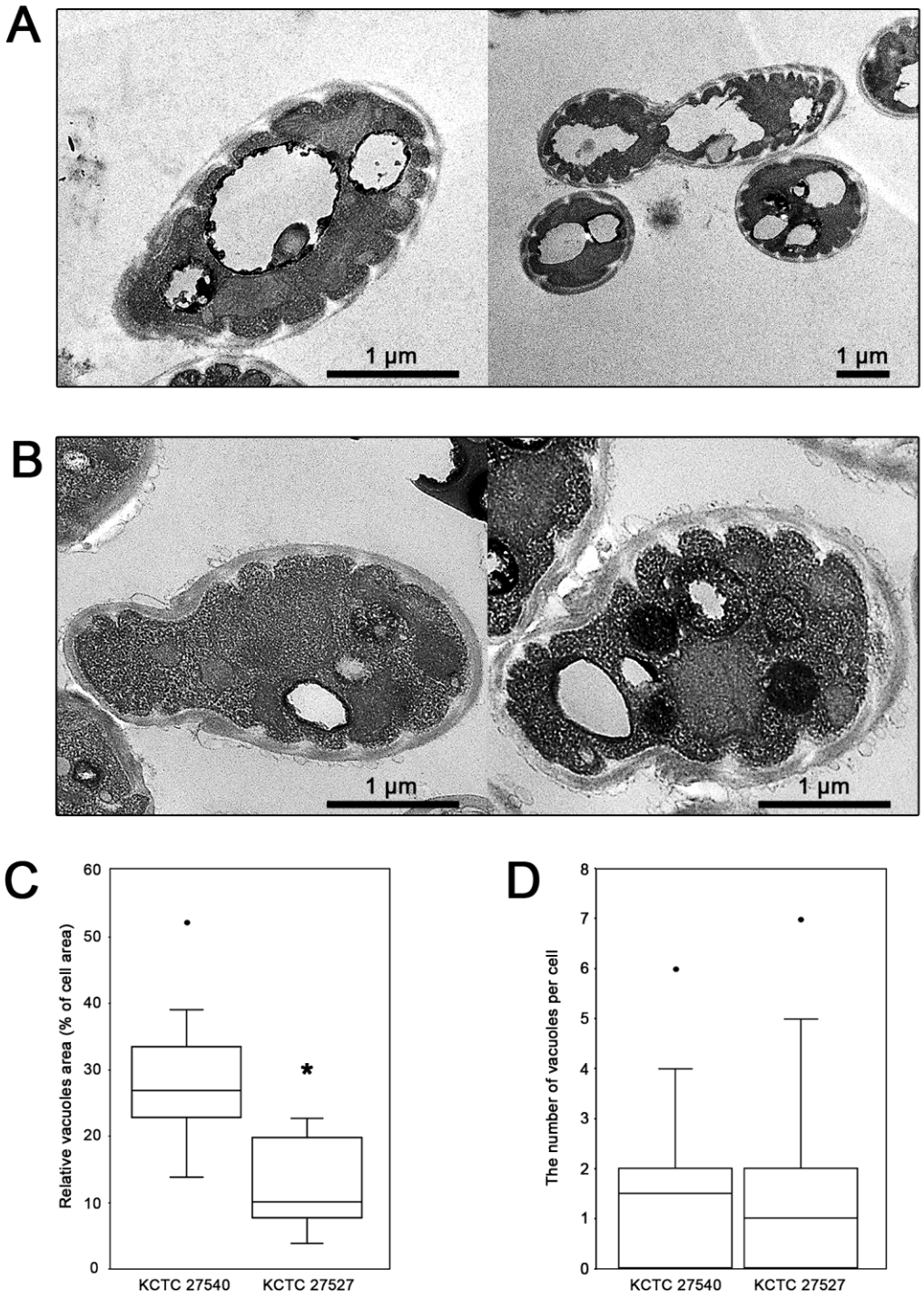

872

873 **Fig. 3. Morphology of vacuoles in *M. restricta* cells containing MrV40.** Ultrathin sections

874 of strains KCTC 27540 (A) and KCTC 27527 (B) were observed by TEM. Cytoplasmic

875 vacuole formation in the strains, expressed as the percentage of cells occupied by vacuoles (n
876 = 20 cells from each strain) (*p < 0.001) (C) and number of vacuoles per cell (n = 30 cells
877 from each strain) (D) were estimated. The measurements were displayed as a box plot
878 including the median values with the upper and lower quartiles. The lines expanded from the
879 boxes represent the minimum and maximum values, and outliers are displayed as dots.

880

881

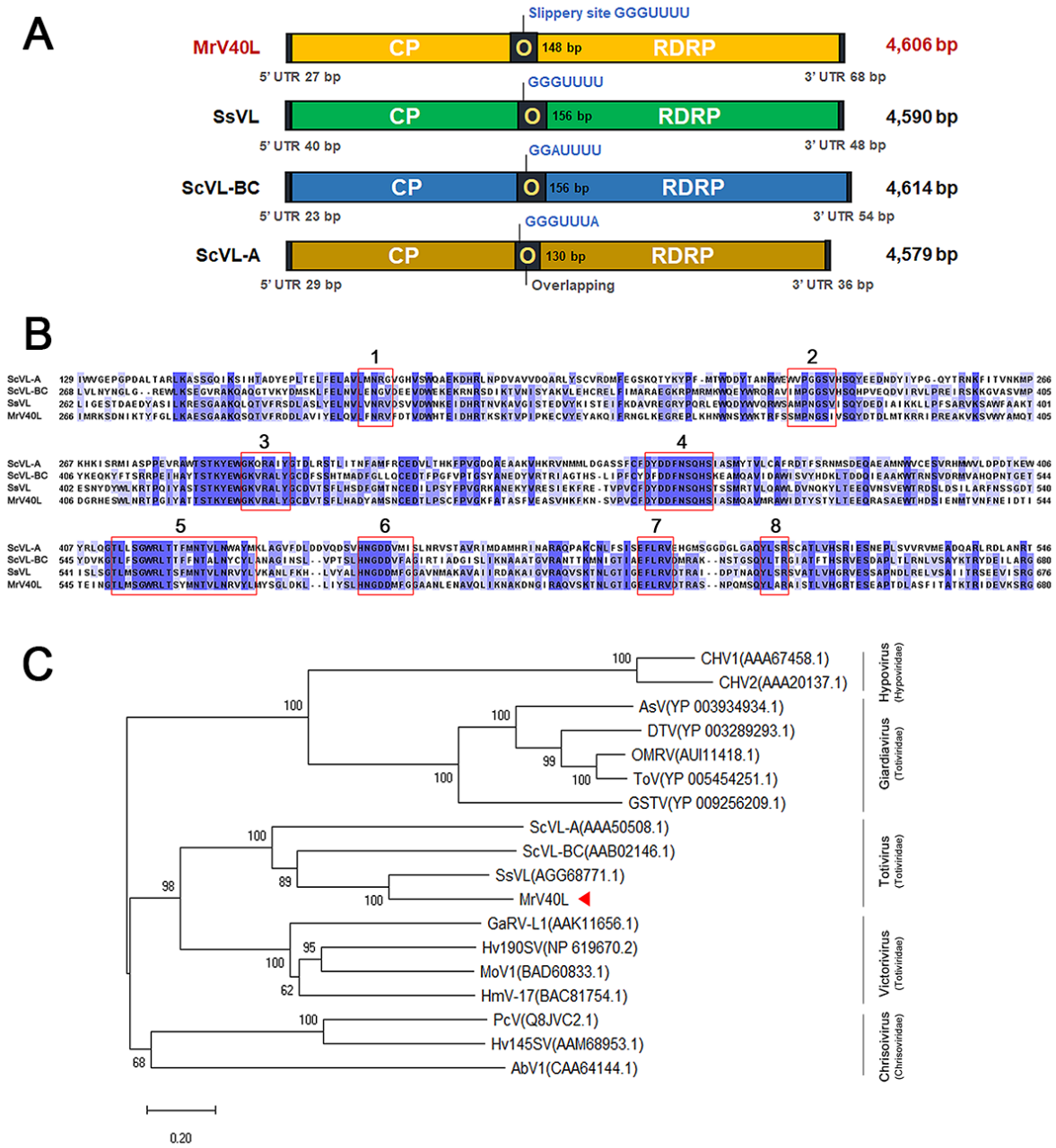

Fig. 4. Genome and phylogenetic analysis of MrV40L. (A) Comparison of the genomic organization of MrV40L with that of other Totiviruses. (B) Eight conserved motifs within the

886 viral RDRP of MrV40L. The red boxes indicate conserved motifs. The amino acid sequences
887 of ScVL-A, ScVL-BC, SsVL, and MrV40L were aligned using Jalview. (D) Multiple
888 alignment of 18 amino acid sequences of RDRPs from dsRNA viruses was analyzed using the
889 neighbor-joining method with bootstrap test (1,000 replicates) using MEGA X (78, 81, 82).
890 The evolutionary distances are in units of the number of amino acid substitutions per site. All
891 ambiguous positions were removed for each sequence pair. CHV1, *Cryphonectria* hypovirus
892 1; CHV2, , *Cryphonectria* hypovirus 2; AsV, *Armigeres subalbatus* virus; DTV, *Drosophila*
893 *melanogaster* totivirus; OMRV, *Omono river* virus; ToV, *Tianjin* totivirus; GSTV, *Golden*
894 *shiner* totivirus; ScVL-A, *S. cerevisiae* virus L-A; ScVL-BC, *S. cerevisiae* virus L-BC; SsVL,
895 *S. segobienesis* virus L; GaRV-L1, *Gremmeniella abietina* virus L1; Hv190SV,
896 *Helminthosporium victoriae* virus-190S; MoV1, *Magnaporthe oryzae* virus 1; HmV-17,
897 *Helicobasidium mompa* totivirus 1-17; PcV, *Penicillium chrysogenum* virus; Hv145SV,
898 *Helminthosporium victoriae* 145S virus; AbV1, *Agaricus bisporus* virus 1 (8, 32, 33, 83-95).

899

900

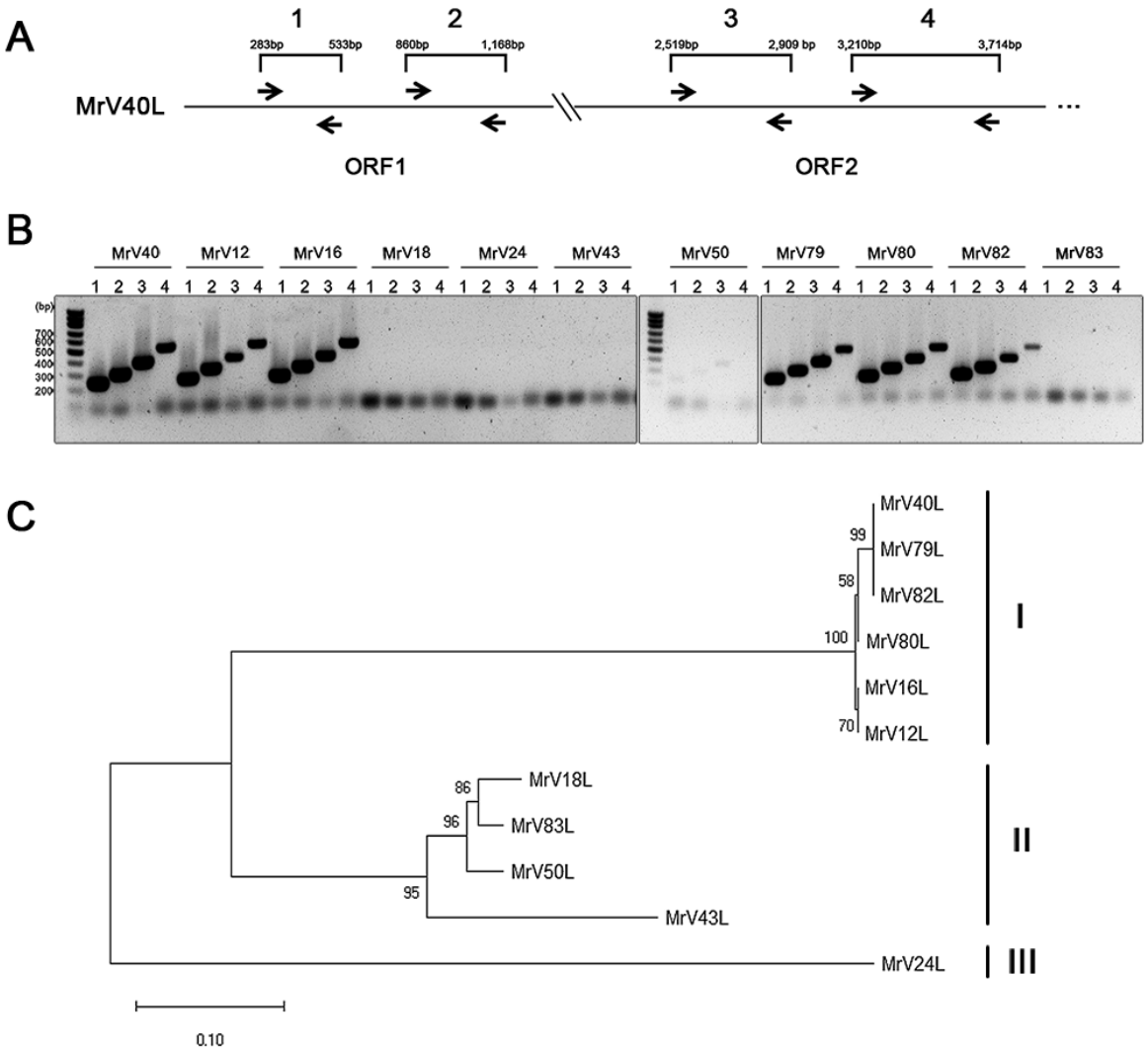

Fig. 5. Phylogenetic classification of viruses found in *M. restricta*. (A, B) The cDNAs of dsRNAs from *M. restricta* strains were amplified using primers for genes encoding CP and RDRP (ORF1 and ORF2, respectively) homologs in the viral genome. The following primers were used: lane 1, MrV40L_CP_F1 and MrV40L_CP_R1; lane 2, MrV40L_CP_F2 and MrV40L_CP_R2; lane 3, MrV40L_RDRP_F1 and MrV40L_RDRP_R1; lane 4,

MrV40L_RDRP_F2 and MrV40L_RDRP_R2 (see Table S2 in supplemental material). (C) MrV-Ls were clustered into three clades (clade I, II, and III). Multiple alignment of nucleotide sequences of combined parts of *gag* and *pol* from 11 MrV-Ls was analyzed by the neighbor-joining method with bootstrap test (1,000 replicates) in MEGA X (78, 81, 82). The evolutionary distances are in units of the number of base substitutions per site.

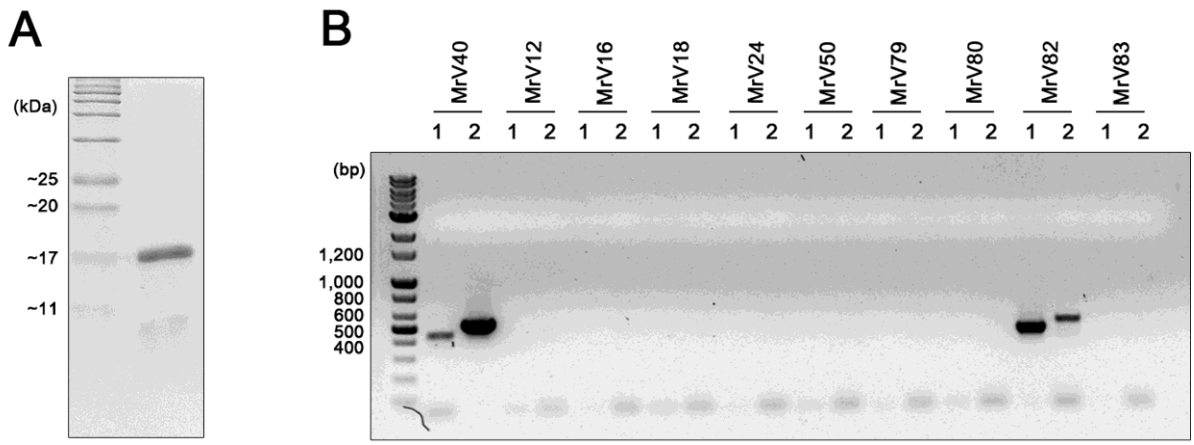

916

917

918

919 **Fig. 6. Characterization and similarity analysis of MrV40S.** (A) The protein encoded by
920 ORF3 was heterologously expressed in *E. coli* and purified using a His-tag column. (B) RT-
921 PCR results. The primers specific to MrV40S were used to amplify satellite dsRNA from
922 other *M. restricta* strain containing small dsRNA segments. The following primers were used:
923 lane 1, MrV40S_F5 and V40S_SP1; lane 2, MrV40S_ORF_F1 and MrV40S_R1 (see Table
924 S2 in supplemental material).

925

926

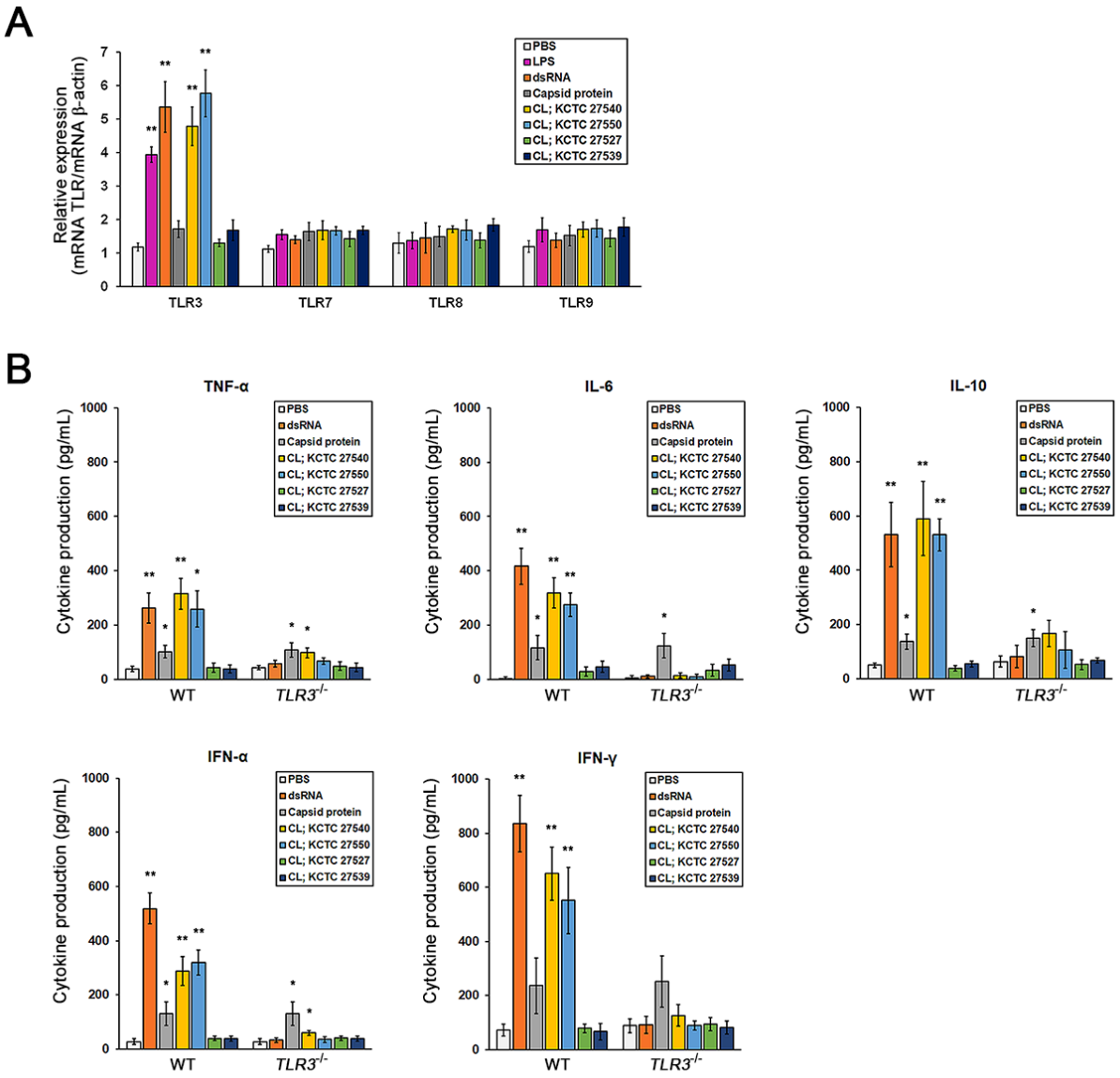

Fig. 7. Evaluation of *TLR* and cytokine levels upon treatment with the viral elements. *TLR* expression (A) and cytokines production (B) in BMDCs co-incubated with purified MrV40 dsRNA, purified capsid protein of MrV40, and total cell lysates of the *M. restricta* strains containing the virus (KCTC 27540 and KCTC 27550) and virus-free *M. restricta* strains (KCTC 27527 and KCTC 27539). PBS and lipopolysaccharide served as the negative and positive controls, respectively. WT; wild- type mice (C57BL/6), *TLR3*$^{-/-}$; *TLR3* knock out mice (B6;129S1-Tlr3^{tm1Flv}/J, 005217), CL; cell lysate. (*p < 0.01 and **p < 0.001).